

See discussions, stats, and author profiles for this publication at: <https://www.researchgate.net/publication/6664347>

# Tetrabromocinnamic Acid (TBCA) and Related Compounds Represent a New Class of Specific Protein Kinase CK2 Inhibitors

ARTICLE *in* CHEMBIOCHEM · JANUARY 2007

Impact Factor: 3.09 · DOI: 10.1002/cbic.200600293 · Source: PubMed

CITATIONS

79

READS

42

12 AUTHORS, INCLUDING:



**Mario Angelo Primo Pagano**

University of Padova

52 PUBLICATIONS 1,531 CITATIONS

SEE PROFILE



**Giorgio Cozza**

University of Padova

64 PUBLICATIONS 1,151 CITATIONS

SEE PROFILE



**Maria Ruzzene**

University of Padova

95 PUBLICATIONS 3,566 CITATIONS

SEE PROFILE



**Stefania Sarno**

University of Padova

94 PUBLICATIONS 3,505 CITATIONS

SEE PROFILE

# Tetrabromocinnamic Acid (TBCA) and Related Compounds Represent a New Class of Specific Protein Kinase CK2 Inhibitors

Mario A. Pagano,<sup>[a]</sup> Giorgia Poletto,<sup>[a]</sup> Giovanni Di Maira,<sup>[a]</sup> Giorgio Cozza,<sup>[a]</sup> Maria Ruzzene,<sup>[a]</sup> Stefania Sarno,<sup>[a]</sup> Jenny Bain,<sup>[b]</sup> Matthew Elliott,<sup>[b]</sup> Stefano Moro,<sup>[c]</sup> Giuseppe Zagotto,<sup>[c]</sup> Flavio Meggio,<sup>[a]</sup> and Lorenzo A. Pinna<sup>\*[a]</sup>

*Abnormally high constitutive activity of protein kinase CK2, levels of which are elevated in a variety of tumours, is suspected to underlie its pathogenic potential. The most widely employed CK2 inhibitor is 4,5,6,7-tetrabromobenzotriazole (TBB), which exhibits a comparable efficacy toward another kinase, DYRK1a. Here we describe the development of a new class of CK2 inhibitors, conceptually derived from TBB, which have lost their potency toward DYRK1a. In particular, tetrabromocinnamic acid (TBCA) inhibits CK2 five times more efficiently than TBB (IC<sub>50</sub> values 0.11 and*

*0.56  $\mu$ M, respectively), without having any comparable effect on DYRK1a (IC<sub>50</sub> 24.5  $\mu$ M) or on a panel of 28 protein kinases. The usefulness of TBCA for cellular studies has been validated by showing that it reduces the viability of Jurkat cells more efficiently than TBB through enhancement of apoptosis. Collectively taken, the reported data support the view that suitably derivatized tetrabromobenzene molecules may provide powerful reagents for dissecting the cellular functions of CK2 and counteracting its pathogenic potentials.*

## Introduction

Protein kinases, catalysing the phosphorylation of serine, threonine and tyrosine residues in protein substrates, make up a huge superfamily of enzymes (sometimes collectively termed the "kinome"<sup>[1,2]</sup>) that play central roles in controlling nearly all cellular functions. Abnormally elevated activity and/or expression of protein kinases underlie several pathologies, with special reference to neoplasia,<sup>[3]</sup> thus making this class of enzymes the most numerous representatives of the so called druggable genome.<sup>[4,5]</sup> Therefore, the development of efficient, selective and cell-permeable inhibitors of protein kinases not only represents a powerful tool for elucidating the functional implications of individual enzymes, but it might also provide valuable leads for successful drugs.<sup>[4–7]</sup> Nowadays several protein kinase inhibitors have entered clinical practice or are in advanced clinical trials for treatment of tumours and other diseases,<sup>[4,8,9]</sup> the most remarkable example being provided by imatinib (also termed STI-571 or Gleevec), an inhibitor of Abl protein tyrosine kinase that is proving extremely effective for treatment of chronic myelogenous leukaemia.<sup>[10]</sup>

The Ser/Thr-specific protein kinase CK2 (an acronym derived from the misnomer "casein kinase-2") is probably the most pleiotropic member of the human kinome, with more than 300 protein substrates identified so far, the majority of them implicated in signal transduction, gene expression, DNA repair, RNA and protein synthesis.<sup>[11]</sup> Unlike the majority of protein kinases, which are turned on only in response to specific stimuli, the catalytic subunits of CK2 ( $\alpha$  and/or  $\alpha'$ ) are constitutively active either alone or in combination with the regulatory  $\beta$  subunits to give heterotetrameric holoenzymes ubiquitously expressed

in all types of eukaryotic cells.<sup>[12–15]</sup> Given such insensitivity to any known physiological effector(s), the most valuable tool for dissecting the cellular functions of CK2 is the development of highly specific, cell-permeable inhibitors. In perspective, these compounds could display pharmacological potential as well, in view of a number of coincidental arguments and experimental models strongly suggesting that the catalytic activity of CK2 can under certain circumstances be responsible for the enhancement of the tumour phenotype.<sup>[16,17]</sup> CK2 is in fact invariably elevated in a wide spectrum of tumours,<sup>[16]</sup> and unscheduled expression of CK2 catalytic subunits displays an oncogenic potential in a number of cellular and animal models.<sup>[18–21]</sup> The increasingly widely accepted concept is that CK2 is strong-

[a] Dr. M. A. Pagano, Dr. G. Poletto, Dr. G. Di Maira, Dr. G. Cozza, Dr. M. Ruzzene, Dr. S. Sarno, Prof. F. Meggio, Prof. L. A. Pinna  
Department of Biological Chemistry and CNR Institute of Neurosciences  
University of Padova  
viale G. Colombo 3, 35121 Padova (Italy)  
Fax: (+39) 049-8073310  
E-mail: lorenzo.pinna@unipd.it

[b] Dr. J. Bain, Dr. M. Elliott  
Medical Research Council Protein Phosphorylation Unit  
University of Dundee  
Dundee DD1 5EH (UK)

[c] Prof. S. Moro, Prof. G. Zagotto  
Department of Pharmaceutical Sciences, Molecular Modeling Section  
University of Padova  
via Marzolo 5, 35121 Padova, Italy

Supporting information for this article is available on the WWW under <http://www.chembiochem.org> or from the author.

ly committed to cell survival<sup>[17,22]</sup> and that to achieve this goal it plays a global anti-apoptotic role. This makes it a potential target for anti-neoplastic therapies designed to combat those kinds of tumours in which malignancy is primarily due to dys-regulated apoptosis.<sup>[17,23,24]</sup>

A number of CK2 inhibitors effective in the low micromolar and submicromolar ranges have been described so far. They belong to three main classes: 1) condensed polyphenolic compounds exemplified by emodin<sup>[25]</sup> and its improved derivatives,<sup>[26]</sup> 2) brominated benzimidazole/triazole derivatives,<sup>[27]</sup> and 3) derivatives of indolo quinazolines, exemplified by IQA.<sup>[28,29]</sup> A few flavonoids, notably quercetin and apigenin, should also be included in the repertoire of CK2 inhibitors, though these tend to be rather promiscuous, inhibiting a large spectrum of protein kinases other than CK2.<sup>[29,30]</sup> Up to now the most successful and widely used CK2 inhibitor is probably TBB (tetrabromobenzotriazole), which has been employed to verify the implication of CK2 in the phosphorylation of a variety of endogenous proteins (reviewed by Sarno<sup>[31]</sup>) and to induce apoptosis of tumour cell lines.<sup>[17,32,33]</sup> In vitro, TBB and its congener, which contains an imidazole moiety in place of the triazole ring, display  $IC_{50}$  values of between 0.5–1  $\mu$ M, with small, yet significant, differences in terms of their efficacy toward CK2 holoenzyme as compared to the isolated catalytic subunits and possibly of their cell permeability.<sup>[34]</sup> The efficacy of TBB, both in vitro and in cell cultures, has been improved by generating adducts in which N2 is replaced by a carbon atom bound to a variety of polar functions.<sup>[27]</sup> The most efficient derivative, DMAT (also termed 2c or K25), bears a dimethylamino group bound to position 2 of the 4,5,6,7-tetrabromobenzimidazole scaffold and displays an  $IC_{50}$  value of 0.14  $\mu$ M.<sup>[27,35]</sup> The crystal structures of TBB and three TBB derivatives (including DMAT/K25), as well as those of IQA, emodin and three emodin derivatives in complexation with the catalytic subunit of CK2, have been solved, revealing, in conjunction with mutational analysis, the crucial role of a number of hydrophobic residues, the bulkiness of which makes a hydrophobic cavity adjacent to the ATP binding site smaller in CK2 than in it is in the majority of other protein kinases.<sup>[29,36–39]</sup> This is likely to account for the fairly narrow selectivity of CK2 inhibitors, several of which are much less effective with a repertoire of more than 30 different protein kinases. A remarkable exception, however, is provided by DYRK1a, a kinase implicated in neurological disorders,<sup>[40–42]</sup> the susceptibility of which to most

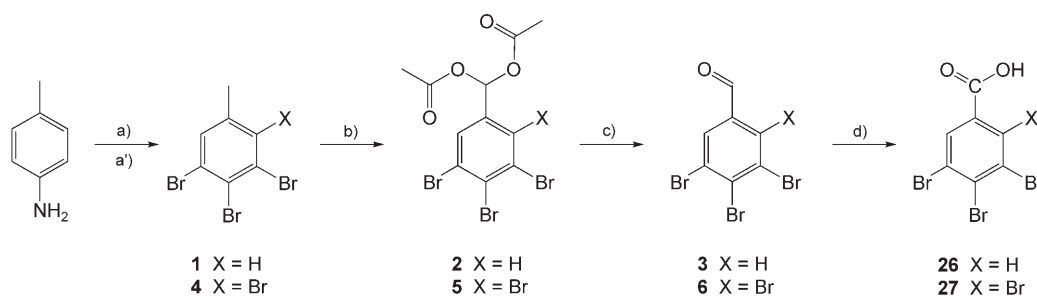
CK2 inhibitors, with special reference to TBB and its derivatives, is comparable to, if not even higher than, that of CK2.<sup>[27,29]</sup>

Although the high-affinity binding of TBB derivatives is stabilized by apolar contacts between the hydrophobic pocket of CK2 and the inhibitor molecule, with special reference to its tetrabrominated benzene ring, the orientation of the ligand and its occupancy of the hydrophobic cavity are determined by weak polar interactions involving the negatively charged triazole ring of TBB and the polar groups of some of its derivatives.<sup>[39]</sup> This state of affairs prompted us to try to design a new class of CK2 inhibitors in which the tetrabrominated benzene ring is conserved while the adjacent rigid pentaatomic ring is opened, thus becoming a flexible “tether” that can be functionalised with polar groups. Consequently, the apolar ring and the polar tether, if properly tailored, should be able to adopt the most stable positions independently of each other, with an overall larger drop in free energy. To this purpose a small library of compounds sharing the feature of a variably brominated benzene ring and differing in the nature, length and position of the side chain has been synthesized and each compound has been assayed for its ability to inhibit CK2 and possibly additional kinases, with special reference to DYRK1a, which is inhibited as efficiently as CK2 by TBB and its derivatives. This investigation, described here, has resulted in the identification of a novel class of inhibitors that specifically affect CK2 without comparable efficacy on DYRK1a. One of these new compounds, moreover, is more potent than TBB both in vitro and in vivo.

## Results and Discussion

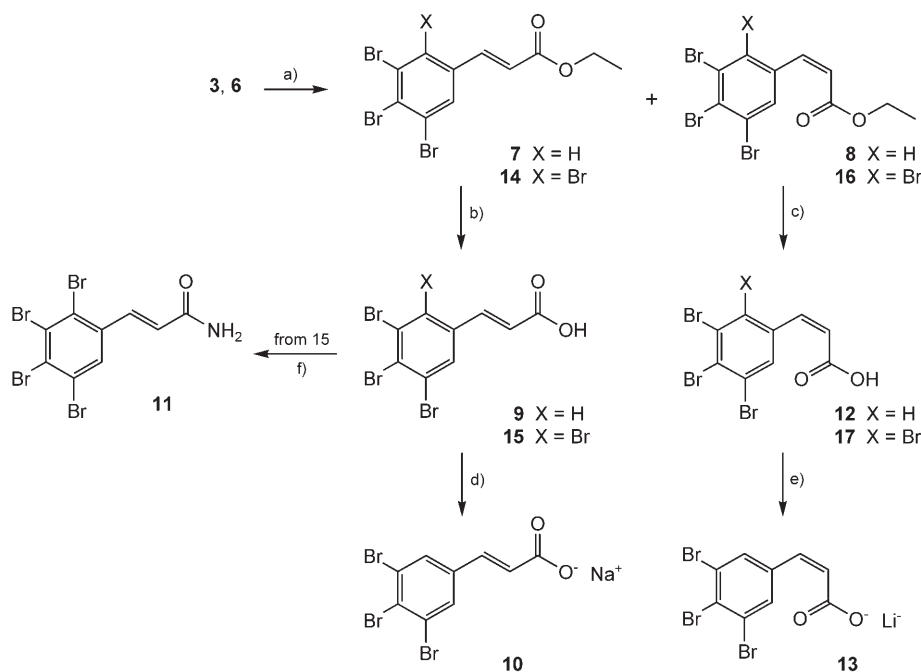
### Chemistry

With the aim of finding small molecules that might target the protein kinase CK2 as good inhibitors in the nanomolar range we synthesized a series of tri- and tetrabromo derivatives that have structural simplicity as a common feature. The general procedure consisted of the preparation of the polybromoaldehydes, which were subsequently treated, often in a Wittig reaction, to give the corresponding acrylate derivatives. In the first instance only the synthesis of the polybromoaldehydes is reported (Scheme 1), since it was known that the presence of three or more bromine substituents on the aromatic ring was necessary to inhibit the enzyme to a significant extent. The

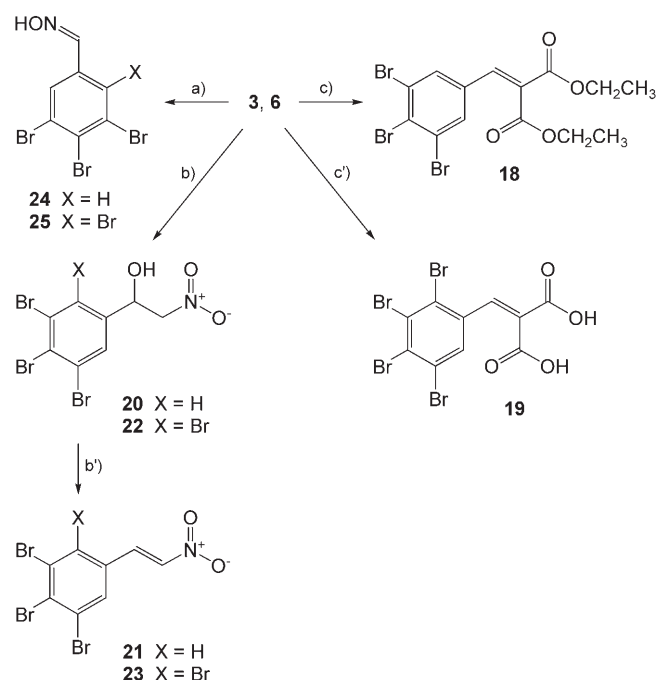


**Scheme 1.** Synthesis of polybromobenzaldehydes and polybromobenzoic acids. Reagents: a)  $Br_2$ ,  $CuBr_2$ ,  $(CH_3)_3CONO$ , acetonitrile [(a')  $Br_2$ ,  $I_2$ , RT, 7 d]; b)  $CrO_3$ ,  $(CH_3CO)_2O$ ,  $H_2SO_4$ ,  $0^\circ C$ , 20 h; c)  $H_2SO_4$ , reflux, 2 h,  $H_2O/EtOH$ ; d)  $KMnO_4$ , reflux, 2 h, dil.  $H_2SO_4$ .

corresponding acrylic derivatives were then obtained and the *E* and *Z* isomers were separated by column chromatography (Scheme 2).



**Scheme 2.** Synthesis of (polybromophenyl)acrylic acid derivatives. Reagents: a)  $(\text{Ph})_3\text{PCHCOOEt}$ , from  $0^\circ\text{C}$  to  $10^\circ\text{C}$ , 45 min.,  $\text{CH}_2\text{Cl}_2$ ; b)  $\text{NaOH}$ ,  $50^\circ\text{C}$ , 2 h,  $\text{EtOH}/\text{THF}/\text{H}_2\text{O}$ ; c)  $\text{LiOH}$ , RT, 12 h,  $\text{THF}/\text{H}_2\text{O}$ ; d)  $\text{NaOH}$ ,  $50^\circ\text{C}$ , 30 min.,  $\text{H}_2\text{O}$ ; e)  $\text{LiOH}$ ,  $50^\circ\text{C}$ , 2 h,  $\text{H}_2\text{O}$ ; f)  $\text{SOCl}_2$ , reflux, 1 h,  $\text{CH}_2\text{Cl}_2$  then  $\text{NH}_4\text{OH}$ ,  $20^\circ\text{C}$ , 1 h, dioxane.



**Scheme 3.** Synthesis of oximes and malonic ester and nitromethane derivatives of polybromobenzaldehydes. Reagents: a)  $\text{NH}_2\text{OH}\cdot\text{HCl}$ ,  $\text{EtOH}/\text{pyridine}$ ; b)  $\text{CH}_3\text{NO}_2$ ,  $t\text{BuOK}$ ,  $\text{THF}/t\text{BuOH}$ ; b')  $\text{CH}_3\text{SO}_2\text{Cl}$ ,  $\text{CH}_2\text{Cl}_2$ ,  $\text{Et}_3\text{N}$ ; c)  $\text{CH}_2(\text{CO}_2\text{C}_2\text{H}_5)_2$ , piperidine benzoate, toluene, reflux, 4 h; c') malonic acid, acetic acid, 2 h, RT.

The polybromoaldehydes were finally treated with different nucleophiles to provide a set of compounds (Scheme 3) that allowed us to explore the conformational space within the ATP

site of the kinase. The *E/Z* conformations of the oxime derivatives were established by NOESY experiments.

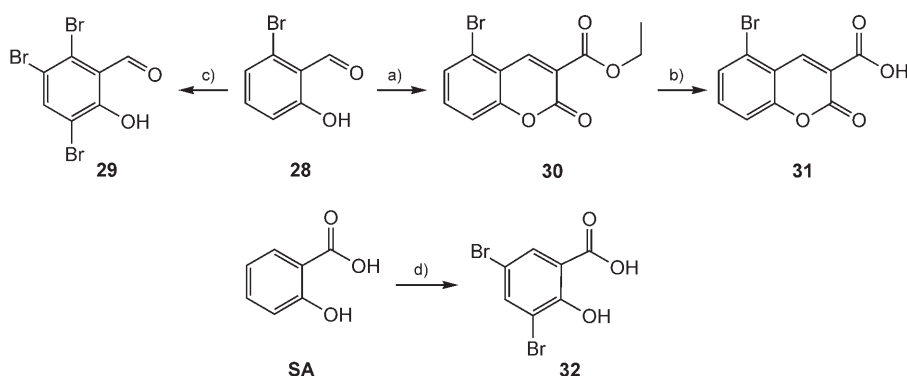
Lastly, to constrain the structure of the cinnamic acid, a coumarin derivative, together with some other derivatives of salicylic acid, was synthesized as shown in Scheme 4.

### In vitro biological data

The library of tethered derivatives of brominated benzene used in this study is displayed in Table 1, where the  $\text{IC}_{50}$  values for their inhibition of CK2 are also reported. It can be seen that 18 out of the 35 compounds considered significantly inhibit CK2 activity at concentrations  $<40\text{ }\mu\text{M}$ . Four of these—**9**, **10**, **15** and **26**—display  $\text{IC}_{50}$  values  $<1\text{ }\mu\text{M}$ . Interestingly, none of them inhibits DYRK1a to a comparable extent, their  $\text{IC}_{50}$  values all being one to two orders of

magnitude higher in this case (Table 2). Rat liver CK1 is entirely insensitive to all the compounds listed in Table 1, tested up to  $40\text{ }\mu\text{M}$  (not shown).

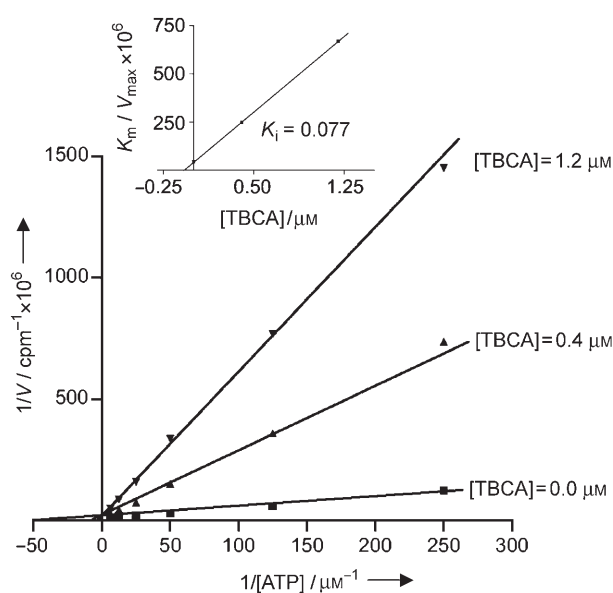
The most remarkable compound appears to be **15**, tetrabromocinnamic acid (henceforth denoted as TBCA), with an  $\text{IC}_{50}$  value of just  $0.11\text{ }\mu\text{M}$ , the lowest reported so far for a CK2 inhibitor and more than 200 times lower than that calculated for the same compound with DYRK1a. As in the case of TBB and TBB-related compounds, TBCA inhibits CK2 competitively with respect to ATP (see Figure 1). From the kinetics shown in Figure 1 the  $K_i$  value of TBCA was calculated to be  $77\text{ nM}$ , a value similar to that of DMAT/2c, but that compound, however, inhibits DYRK1a even more efficiently than it does CK2.<sup>[27,35]</sup> To provide an overall evaluation of TBCA selectivity this compound was tested on a panel of 28 kinases at  $10\text{ }\mu\text{M}$  concentration, and the results reported in Table 3 show that, while CK2 activity is entirely suppressed, all the other kinases are either unaffected or only partially inhibited by TBCA, the only kinases to be inhibited by more than 50% being SGK and GSK3 $\beta$ , the activities of which are reduced by about 70%. As shown in Figure 2, however, the  $\text{IC}_{50}$  value of GSK3 $\beta$ , determined under comparable conditions ( $0.1\text{ mM}$  ATP concentration in both cases), is 12 times higher than that of CK2. Such a difference, as clearly outlined in Figure 2, is sufficient to discriminate neatly between CK2 and GSK3 $\beta$  activities in vitro and, by extrapolation, in cultured cells as well.



**Scheme 4.** Synthesis of coumarin and salicylic acid derivatives. Reagents: a)  $\text{CH}_2(\text{COOEt})_2$ , piperidine, reflux, 24 h,  $\text{CH}_3\text{COOH}/\text{EtOH}$ ; b)  $\text{NaOH}$ , reflux, 2 h,  $\text{H}_2\text{O}$ ; c)  $\text{NBS}$ ,  $\text{CCl}_4$ ; d)  $\text{NBS}$ , from  $0^\circ\text{C}$  to  $25^\circ\text{C}$ , 16 h, acetonitrile.

mines, and even more so if **32** (3,5-dibromo-2-hydroxybenzoic acid) is compared with salicylic acid (SA, 2-hydroxybenzoic acid): while the former compound is still a fairly good inhibitor ( $\text{IC}_{50} = 3.83\ \mu\text{M}$ ), the latter is no longer an inhibitor at all.

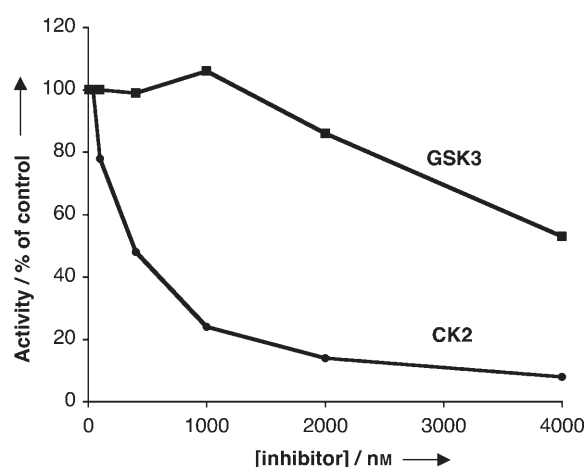
The relevance of apolar interactions is corroborated by the effect of the mutation of two unique bulky residues—V66 and I174—inside the hydrophobic pocket of CK2: mutation of these residues to alanines, which



**Figure 1.** Lineweaver–Burk inhibition plots of protein kinase CK2 by TBCA. CK2 activity was determined as described in the Experimental Section either in the absence or in the presence of the indicated concentration of inhibitor. The data represent means of experiments run in triplicate with SE never exceeding 10%. The inset shows the  $K_m/V_{\text{max}}$  vs.  $[I]$  replot from which the value of  $K_i$  has been determined.

A comparison between the compounds listed in Table 1 allows some conclusions to be drawn about the structural features that make TBCA an especially potent inhibitor of CK2. The crucial relevance of the negatively charged carboxylic group at the end of its side chain is highlighted by the loss of inhibitory power observed upon its methylation (compare TBCA with **14**) and by the drop in inhibition promoted by its amidation (compare TBCA with **11**). The orientation of the carboxylic group is also important, since **17**, the *cis* stereoisomer of TBCA, displays an  $\text{IC}_{50}$  value  $> 30$  times higher.

The presence of multiple bromines on the benzene ring also represents a necessary—though not sufficient—condition for efficient CK2 inhibition in this new series of inhibitors, as becomes clear if the inhibitory power of the tetrabromo derivatives is compared to that of congeners with just three bro-

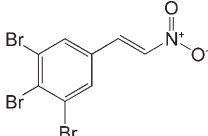
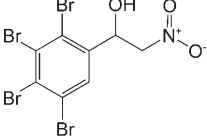
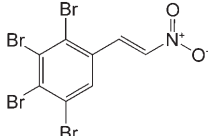
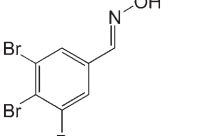
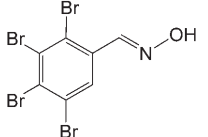
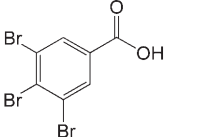
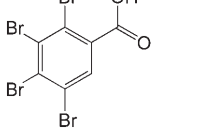
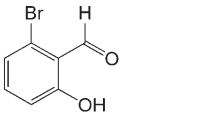
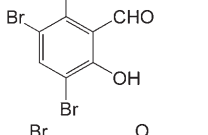
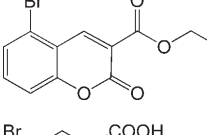
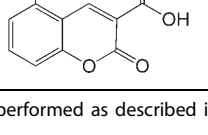
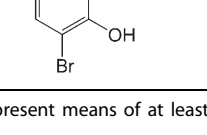


**Figure 2.** Dose-dependent inhibition of protein kinases CK2 and GSK3 by TBCA. The activities of CK2 and GSK3 $\beta$  were determined by incubation, as described in the Experimental Section, of 0.5–1 pmol of each kinase in the presence of increasing concentrations of TBCA. To obtain comparable results the protein phosphatase inhibitor 2 was used as common phosphorylatable substrate and identical concentrations of ATP (0.1 mM) were present in the assays.  $\text{IC}_{50}$  values of 0.35 and  $4.25\ \mu\text{M}$  were calculated for CK2 and GSK3 $\beta$ , respectively. The data were obtained from the autoradiograms after SDS-PAGE and represent the means of three independent experiments.

dramatically impairs the inhibitory power of TBB and TBB derivatives,<sup>[31,39]</sup> also adversely affects inhibition by TBCA and even more so by some related compounds (Table 4), consistently with the concept that the same hydrophobic pocket that harbours TBB and its derivatives is also implicated in the interaction with these novel CK2 inhibitors. Interestingly, however, TBCA is less sensitive to this mutation than TBB and DMAT, with just a fivefold increase in  $\text{IC}_{50}$  (Table 4), as compared to 25- and 41-fold, respectively, suggesting that the flexibility of the acrylic “tail” of TBCA allows its brominated benzene ring to move in order to produce van der Waals interactions with residues other than V66 and I174, if these are absent. Two observations are consistent with this interpretation: firstly, the TBCA analogue **9**, possessing an identical acrylic side chain and differing in the lack of one of the four bromines, is also poorly sensitive to the V66/I174 to Ala mutation,

**Table 1.** IC<sub>50</sub> values of variably substituted bromobenzene derivatives for protein kinase CK2.

Compound	Structure	IC <sub>50</sub> [μM] <sup>[a]</sup>	Compound	Structure	IC <sub>50</sub> [μM] <sup>[a]</sup>
SA (salicylic acid)		> 40.00	PAS		> 40.00
1		> 40.00	2		15.00 ± 0.62
3		30.00 ± 0.84	4		> 40.00
5		4.93 ± 0.25	6		16.90 ± 0.77
7		> 40.00	8		> 40.00
9		0.73 ± 0.06	10		0.78 ± 0.02
11		3.01 ± 0.31	12		> 40.00
13		23.50 ± 1.28	14		> 40.00
15 (TBCA)		0.11 ± 0.01	16		> 40.00
17		3.38 ± 0.07	18		> 40.00
19		33.66 ± 1.45	20		> 40.00

Table 1. (Continued)					
Compound	Structure	IC <sub>50</sub> [μM] <sup>[a]</sup>	Compound	Structure	IC <sub>50</sub> [μM] <sup>[a]</sup>
21		> 40.00	22		10.77 ± 0.87
23		13.32 ± 0.74	24		18.91 ± 0.59
25		2.45 ± 0.11	26		0.64 ± 0.03
27		13.44 ± 0.40	28		> 40.00
29		> 40.00	30		> 40.00
31		> 40.00	32		3.83 ± 0.08

[a] Activity assays were performed as described in the Experimental Section and the reported data represent means of at least three independent experiments.

Table 2. IC <sub>50</sub> values of the most effective new CK2 inhibitors for protein kinases CK2 and DYRK1 a.		
Inhibitor	IC <sub>50</sub> [μM] for CK2	IC <sub>50</sub> [μM] for DYRK1 a
9	0.73 ± 0.06	12.56 ± 0.97
10	0.78 ± 0.02	17.69 ± 1.82
15 (TBCA)	0.11 ± 0.01	24.50 ± 2.06
26	0.64 ± 0.03	3.50 ± 0.22
TBB	0.50 <sup>[a]</sup>	0.91 <sup>[a]</sup>
DMAT	0.14 <sup>[b]</sup>	0.12 <sup>[b]</sup>
IQA	0.39 <sup>[a]</sup>	8.00 <sup>[a]</sup>

Inhibition constants were calculated as described in the Experimental Section by using the synthetic peptide substrates RRRADDSDDDDD and RRRFRPASPLRGPPK for CK2 and DYRK1 a, respectively. [a] Data taken from ref. [29]. [b] Data taken from ref. [27].

whereas the analogue **26**, differing from **9** only in its shorter and more rigid side chain, perceives the same mutation much more dramatically, with a > 40-fold increase in IC<sub>50</sub>, whilst secondly, unlike in the cases of TBB and TBB derivatives, the crystal structures of which have been solved, attempts to solve the structure of TBCA bound to CK2 were not successful, suggest-

ing that the inhibitor is mobile and may adopt multiple conformations at its binding site. This is also consistent with molecular docking experiments that identified at least two favourable TBCA conformations (Figure 3).

Modelling based on the crystal structures of complexes formed between CK2 and other inhibitors indicates that the negatively charged carboxylic end of the TBCA "tether" interacts with a positively charged area, mainly generated by K68, where previous crystallographic studies<sup>[29,37,39]</sup> have shown that the acetic group of IQA and the triazole ring of TBB, negatively charged at neutral and basic pH,<sup>[34]</sup> are also localized (see Figure 3). From modelling it also appears that the brominated benzene ring of TBCA is more remote from the side chains of V66 and I164 than it is in the case of TBB, consistently with the experimental data in Table 4.

### In-cell biological data

The usefulness of protein kinase inhibitors is also highly dependent on their cell permeabilities, allowing their exploitation to dissect cellular functions affected by the kinase of interest. The majority of previously described CK2 inhibitors, including



**Table 3.** Inhibition of protein kinases by TBCA.

Protein kinase <sup>[a]</sup>	TBCA (10 $\mu$ M)	DMAT <sup>[b]</sup> (10 $\mu$ M)	Protein kinase <sup>[a]</sup>	TBCA (10 $\mu$ M)	DMAT <sup>[b]</sup> (10 $\mu$ M)
MKK1	63 $\pm$ 5	53 $\pm$ 2	MAPK2/ERK2	98 $\pm$ 5	77 $\pm$ 9
JNK/SAPK1c	91 $\pm$ 8	97 $\pm$ 9	SAPK2a/p38	104 $\pm$ 3	85 $\pm$ 9
SAPK2b/p38 $\beta$ 2	78 $\pm$ 4	65 $\pm$ 8	SAPK3/p38 $\gamma$	85 $\pm$ 4	88 $\pm$ 2
SAPK4/p38 $\delta$	80 $\pm$ 1	109 $\pm$ 2	MAPKAP-K1a	84 $\pm$ 3	52 $\pm$ 1
MAPKAP-K2	66 $\pm$ 8	101 $\pm$ 9	MSK1	82 $\pm$ 5	73 $\pm$ 2
PRAK	94 $\pm$ 1	77 $\pm$ 9	PKA	101 $\pm$ 6	80 $\pm$ 2
PKC $\alpha$	86 $\pm$ 7	95 $\pm$ 1	PDK1	67 $\pm$ 9	112 $\pm$ 1
PKB $\alpha$	57 $\pm$ 1	96 $\pm$ 4	SGK	27 $\pm$ 4	29 $\pm$ 4
P70 S6K	54 $\pm$ 8	65 $\pm$ 10	GSK3 $\beta$	28 $\pm$ 3	103 $\pm$ 4
ROCK-II	95 $\pm$ 4	69 $\pm$ 2	AMPK	101 $\pm$ 2	73 $\pm$ 2
CHK1	90 $\pm$ 5	81 $\pm$ 1	CK2	3 $\pm$ 1	28 $\pm$ 1
PHK	67 $\pm$ 1	41 $\pm$ 4	LCK	99 $\pm$ 6	64 $\pm$ 2
CSK	102 $\pm$ 5	109 $\pm$ 4	CDK2/cyclin A	52 $\pm$ 1	20 $\pm$ 1
CK1	48 $\pm$ 1	87 $\pm$ 12	DYRK1a	96 $\pm$ 1	2 $\pm$ 1

[a] Activity assays were linear with respect to time and enzyme concentration under the conditions described or referenced in the Experimental Section. Residual activity, determined in the presence of 10  $\mu$ M inhibitor, is expressed as a percentage of the control performed without inhibitor. [b] Taken from ref. [27].

**Table 4.** IC<sub>50</sub> [ $\mu$ M] values<sup>[a]</sup> for CK2 wt and double mutant (dm) Val66Ile174 AA of selected compounds.

Compound	CK2 wt	CK2 dm	dm/wt
<b>9</b>	0.73	3.00	4.1
<b>15</b> (TBCA)	0.10	0.68	5.0
<b>17</b>	4.00	40.00	10.0
<b>5</b>	5.00	40.00	8.0
<b>26</b>	0.67	29.00	43.2
<b>25</b>	2.45	45.00	18.3
<b>11</b>	3.01	20.70	6.8
<b>32</b>	3.83	27.00	7.0
TBB <sup>[b]</sup>	0.50	12.51	25.02
DMAT <sup>[c]</sup>	0.14	5.79	41.30

[a] The assays were performed in duplicate under conditions described in the Experimental Section. [b] Taken from ref. [26]. [c] Taken from ref. [27].

TBB and its derivatives, are in fact cell-permeable, a property reflected in their abilities to act as powerful pro-apoptotic agents.<sup>[31,32]</sup> In order to assess whether this was also the case for the new class of CK2 inhibitors described here, advantage was taken of Jurkat cells, viability of which has been shown to correlate inversely with the potencies of CK2 inhibitors.<sup>[26,27]</sup> As shown in Figure 4A, the viability of Jurkat cells is reduced by treatment with TBCA more readily than it is by treatment with TBB, consistently with the higher efficacy of TBCA as a CK2 inhibitor in vitro. Parallel experiments showed that cell death correlated with inhibition of endogenous CK2 activity (Figure 4C) and was, at least partially, due to apoptosis, as judged from the degradation of the PARP protein (Figure 4B) and DNA laddering (not shown), both quite evident at 25  $\mu$ M TBCA. The observation that the same concentration of TBCA had a more drastic effect on cell viability (Figure 4A) and CK2 activity (Figure 4C) is consistent with the view that CK2 inhibition also induces cell death by other mechanism(s) besides apoptosis.

## Conclusions

The data presented demonstrate the potentials of a new class of potent and selective CK2 inhibitors derived from TBB (tetrabromobenzotriazole), the inhibitor most commonly exploited to date, through the replacement of the five-atom triazole ring with polar side chains. Unlike TBB and most other known CK2 inhibitors, which display similar potencies with CK2 and DYRK1a, this new class of tethered tetrabromobenzene compounds has no comparable effect on DYRK1a. The main outcomes of this study can be summarized as follows. 1) The potency of TBB and other tetrabromo(azo)benzimidazole compounds widely employed as CK2 inhibitors is not lost upon opening of the five-atom ring if this is replaced by appropriately sized polar side chains. 2) Such "tethered" tetrabromobenzene molecules are more selective and sometimes more potent CK2 inhibitors than TBB itself, as is demonstrated by tetrabromocinnamic acid (**15**, TBCA), the IC<sub>50</sub> value of which is significantly lower than that of TBB, having moreover lost the high inhibitory efficiency toward DYRK1a typical of TBB and TBB derivatives.<sup>[27]</sup> 3) The inhibitory potencies of tethered tetrabromobenzene compounds crucially depend on the lengths and the natures of the side chains, as illustrated by the loss of inhibitory power experienced by TBCA upon methylation of its carboxyl group and by the adverse effect of alteration of the steric conformation of TBCA from *trans* to *cis*. 4) As in the case for TBB, inhibition by TBCA is competitive with respect to ATP, although its mode of binding is significantly different, as suggested both by molecular modelling and by mutational analysis. 5) The new class of CK2 inhibitors described here should be exploitable for in vivo studies, as documented by the ability of TBCA to induce cell apoptosis even more readily than TBB. From this perspective, it might therefore also be possible to develop these compounds into therapeutic tools.



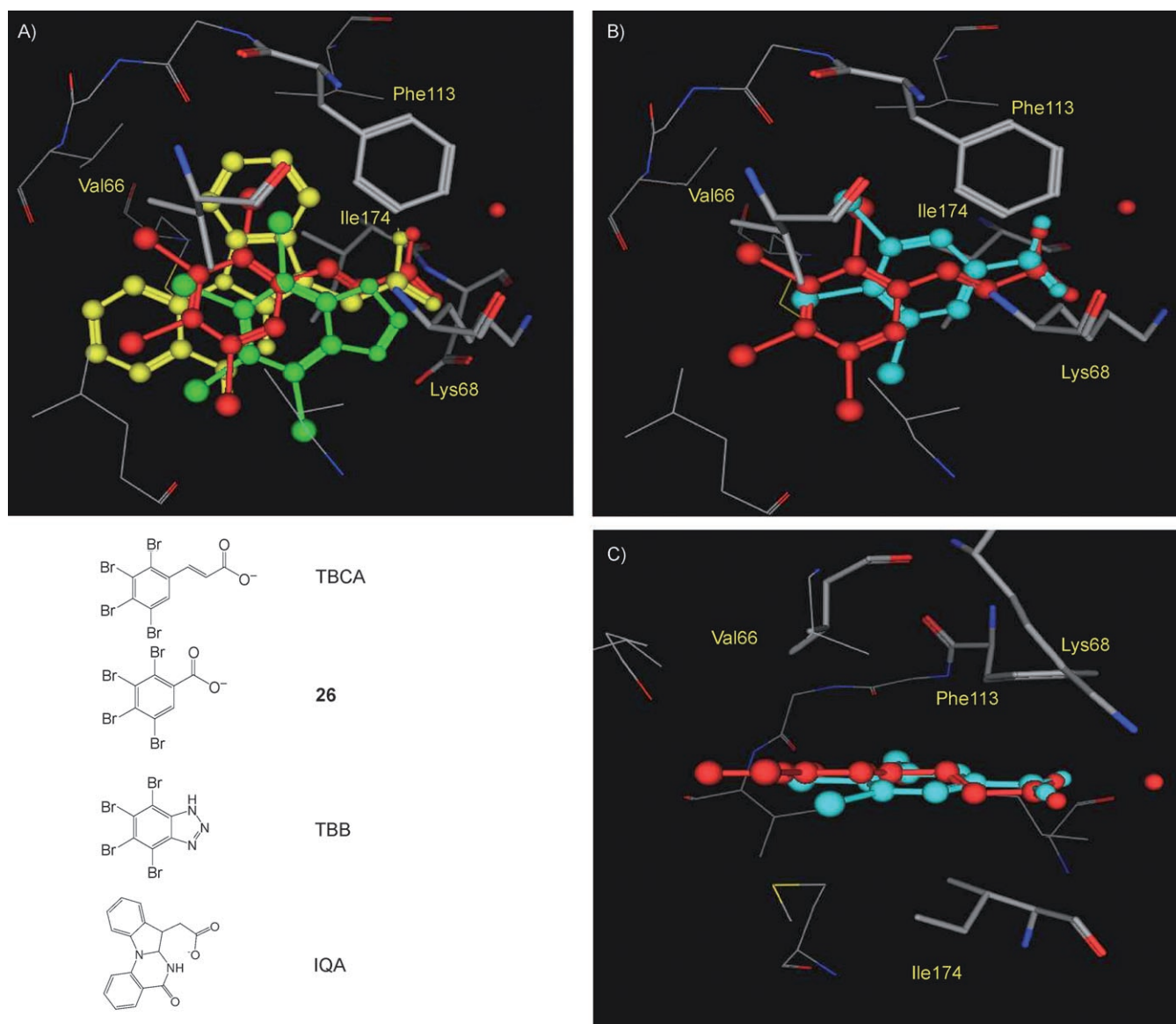


**Figure 3.** Superposition of ATP-binding site directed CK2 inhibitors. A) Superpositions of TBB (green) and IQA (yellow) inhibitors complexed with CK2 $\alpha$  from previous crystallographic studies,<sup>[29,37]</sup> are illustrated together with the best docked conformation of TBCA (red) obtained from computer-assisted molecular modelling. In B and C the different binding of TBCA and **26** (blue) within the CK2 nucleotide pocket is shown as top and lateral view, respectively.

## Experimental Section

**Chemistry:** Melting points were determined in capillary tubes and are uncorrected. Except where noted,  $^1\text{H}$  NMR spectra were obtained in  $\text{CDCl}_3$  or  $[\text{D}_6]\text{DMSO}$  as solvent, or both if necessary to assign the peaks better, and with the solvent peak as internal standard. Nuclear magnetic resonance (NMR) spectra were recorded on a Bruker Avance AMX 250 spectrometer. Chemical shifts are expressed in parts per million relative to tetramethylsilane. Analytical thin-layer chromatography (TLC) was carried out on precoated silica gel plates (Merck 60F<sub>254</sub>), and spots were visualized by use of a UV light (254 nm). Column chromatography was carried out on Merck silica gel (230–400 mesh). All starting materials not described below were purchased from commercial sources. All reagents and solvents were used as received from commercial sources without additional purification. Elemental analysis (CHN) were within 0.4% of the calculated values and were performed on a Carlo-Erba 1016 elemental analyser. Electrospray mass spectra

were obtained with a Mariner API-TOF (Perseptive Biosystems Inc., Framingham MA 01701, USA).

**2,3,4,5-Tetrabromotoluene (4):** This compound was synthesized as described.<sup>[43]</sup> M.p. 112.1–115.3 °C;  $^1\text{H}$  NMR ( $\text{CDCl}_3$ ):  $\delta$  = 2.44 ppm (s, 1 H; arom);  $^{13}\text{C}$  NMR (75 MHz,  $\text{CDCl}_3$ ):  $\delta$  = 24.95, 124.10, 125.60, 127.30, 129.24, 133.20, 140.39 ppm; elemental analysis calcd. (%) for  $\text{C}_7\text{H}_4\text{Br}_4$ : C 20.62, H 0.99, Br 78.39; found: C 20.65, H 1.00, Br 79.01

**2,3,4,5-Tetrabromobenzaldehyde diacetate (5):** 2,3,4,5-Tetrabromotoluene (1.00 g, 2.45 mmol) was dissolved at 0 °C in acetic anhydride (50 mL), and sulfuric acid (0.5 mL) was then dropped in slowly. Chromium trioxide (1.00 g, 6.58 mmol) was added in small portions as the reaction temperature was kept below 10 °C, and the resulting solution was stirred for 2 h at 10 °C, poured into cold water and kept in the fridge for two more hours to complete the precipitation of the product. The suspension was then filtered and

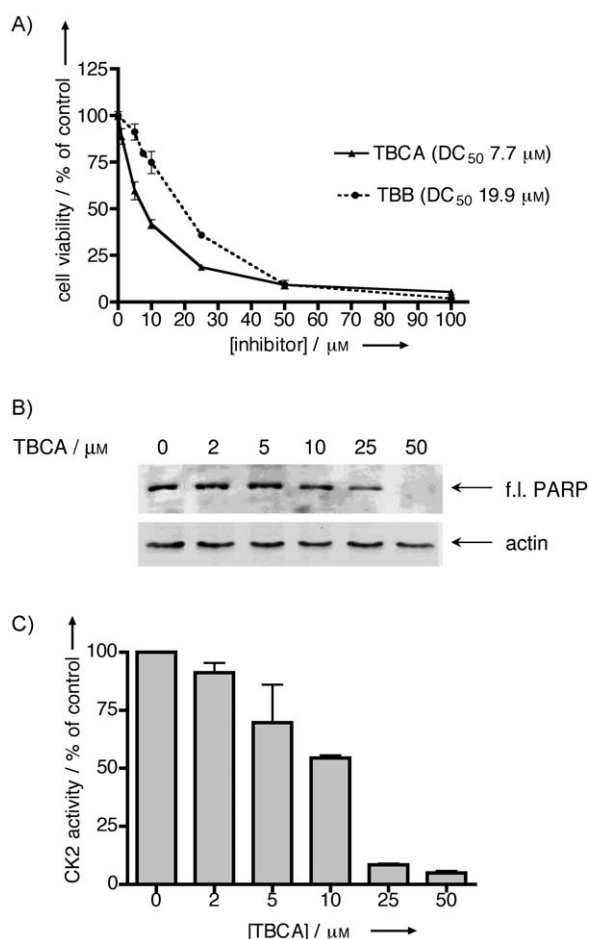


**Figure 4.** Effect of TBCA on cell viability. Jurkat cells were treated for 24 h with increasing concentrations of TBCA or (for comparison) TBB. Control cells were treated with the solvent DMSO (0.5%, v/v). A) Cell viability was assessed by the MTT method, with 100% viability assigned to control cells. The calculated  $\text{DC}_{50}$  values (concentrations required to induce 50% cell death) are indicated. B) Proteins (10  $\mu\text{g}$ ) from cell lysates were analysed by Western blot to assess the caspase-dependent PARP degradation. An antibody recognizing the full-length (f.l.) protein was used. Western blot of actin from the same samples is also shown as a loading control. C) CK2 activity was measured in lysates (1–2  $\mu\text{g}$  proteins) from cells treated with TBCA, with use of the RRRADSDDDDD peptide as substrate, and with 100% activity assigned to control cells. Reported values represent the means  $\pm$  S.E.Ms. from four treatments.

the collected precipitate was washed with water until it became neutral. The solid was then suspended in a cold solution of potassium carbonate in water (2%) and stirred for five minutes. The solid was filtered, washed with water/methanol and dried in a vacuum oven at 35  $^{\circ}\text{C}$ , and the crude product was purified by column chromatography on silica gel (ethyl acetate/hexane 0.9:9.1) to afford the pure **5** in 86% yield.<sup>[44]</sup> M.p. 105.5–107.0  $^{\circ}\text{C}$ ;  $^1\text{H}$  NMR ( $\text{CDCl}_3$ ):  $\delta$  = 2.15 (s, 6H; 2  $\text{CH}_3$ ), 7.76 (s, 1H; arom.), 7.83 ppm (s, 1H; arom.); elemental analysis calcd. (%) for  $\text{C}_{11}\text{H}_8\text{Br}_4\text{O}_4$ : C 25.22, H 1.54, Br 61.02; found: C 25.20, H 1.53, Br 60.95

**2,3,4,5-Tetrabromobenzaldehyde (6):** 2,3,4,5-Tetrabromobenzaldehyde diacetate (0.50 g, 0.95 mmol) was suspended in a mixture of water (37 mL) and ethanol (25 mL), conc. sulfuric acid (1.7 mL) was then slowly dropped in, and the solution was heated at reflux for 2 h and then cooled at 4  $^{\circ}\text{C}$ . The crystals were filtered, washed with water and dried, and the crude product was purified by column

chromatography on silica gel (*n*-hexane) to give the pure **6** in 97% yield.<sup>[43]</sup> M.p. 185.3–187.0  $^{\circ}\text{C}$ ;  $^1\text{H}$  NMR (300 MHz,  $[\text{D}_6]\text{DMSO}$ ):  $\delta$  = 8.12 (s, 1H; arom.), 10.24 ppm (s, 1H; CHO); elemental analysis calcd. (%) for  $\text{C}_7\text{H}_3\text{Br}_4\text{O}$ : C 19.94, H 0.48, Br 75.79; found: C 19.95, H 0.48, Br 75.88.

**Ethyl (*E*)- and (*Z*)-3-(2,3,4,5-tetrabromophenyl)acrylate (14, 16):** 2,3,4,5-Tetrabromobenzaldehyde (**6**, 0.159 g, 0.38 mmol) was added at 0  $^{\circ}\text{C}$  to a solution of (carbethoxymethylene)triphenylphosphorane (159 mg, 0.38 mmol) in dichloromethane (10 mL). The reaction mixture was stirred for 45 min. with the temperature kept below 10  $^{\circ}\text{C}$ , the solvent was then evaporated, and the two isomers were separated by column chromatography on silica gel (toluene/*n*-hexane 30:70). Ethyl (*E*)-3-(2,3,4,5-tetrabromophenyl)acrylate (**14**) was obtained in 68% yield. M.p. 147.3–149.1  $^{\circ}\text{C}$ ;  $^1\text{H}$  NMR (300 MHz,  $\text{CDCl}_3$ ):  $\delta$  = 1.34 (t,  $J$  = 7.1 Hz, 3H;  $\text{OCH}_2\text{CH}_3$ ), 4.29 (q,  $J$  = 7.1 Hz, 2H;  $\text{OCH}_2\text{CH}_3$ ), 6.33 (d,  $J$  = 15.8 Hz, 1H; Ph-CH=CH-), 7.80 (s, 1H; arom.), 7.91 ppm (d,  $J$  = 15.8 Hz, 1H; Ph-CH=CH-);  $^{13}\text{C}$  NMR (75 MHz,  $\text{CDCl}_3$ ):  $\delta$  = 14.21, 60.97, 123.58, 124.93, 126.84, 129.89, 130.15, 130.54, 136.93, 142.25, 165.45 ppm; elemental analysis calcd. (%) for  $\text{C}_{11}\text{H}_8\text{Br}_4\text{O}_2$ : C 26.87, H 1.64, Br 64.99; found: C 26.83, H 1.65, Br 64.88.

**Z Isomer 16:** This isomer was obtained in 24% yield. M.p. 123.6–125.1  $^{\circ}\text{C}$ ;  $^1\text{H}$  NMR (300 MHz,  $\text{CDCl}_3$ ):  $\delta$  = 1.21 (t,  $J$  = 7.1 Hz, 3H;  $\text{OCH}_2\text{CH}_3$ ), 4.13 (q,  $J$  = 7.1 Hz, 2H;  $\text{OCH}_2\text{CH}_3$ ), 6.07 (d,  $J$  = 12.0 Hz, 1H; Ph-CH=CH-), 6.92 (dd,  $J$  = 12.0, 0.6 Hz, 1H; Ph-CH=CH-), 7.66 ppm (d,  $J$  = 0.6 Hz, 1H; arom. H);  $^{13}\text{C}$  NMR (75 MHz,  $\text{CDCl}_3$ ):  $\delta$  = 14.01, 60.69, 123.05, 123.86, 124.85, 128.26, 129.20, 133.05, 138.02, 141.07, 164.71 ppm; elemental analysis calcd. (%) for  $\text{C}_{11}\text{H}_8\text{Br}_4\text{O}_2$ : C 26.87, H 1.64, Br 64.99; found: C 26.87, H 1.66, Br 64.91.

**(*E*)-3-(2,3,4,5-Tetrabromophenyl)acrylic acid (15):** Ethyl (*E*)-3-(2,3,4,5-tetrabromophenyl)acrylate (**14**, 20 mg, 0.04 mmol) was dissolved in THF (20 mL) and aqueous NaOH (32 mg, 0.8 mmol in 5 mL) was then added. The reaction mixture was stirred for 3 h at room temperature, the solvent was evaporated under reduced pressure, the residue was suspended in water and extracted with DCM, the aqueous phase was acidified and extracted again with DCM, the organic phase was dried, and the solvent was evaporated under reduced pressure to leave the 3-(2,3,4,5-tetrabromophenyl)acrylic acid (**15**) in quantitative yield. M.p. 189.2–191.2  $^{\circ}\text{C}$ ;  $^1\text{H}$  NMR ( $\text{CDCl}_3$ ):  $\delta$  = 6.35 (d,  $J$  = 15.8 Hz, 1H; Ph-CH=CH-), 7.82 (s, 1H; arom. H), 8.02 ppm (d,  $J$  = 15.8 Hz, 1H; Ph-CH=CH-);  $^1\text{H}$  NMR ( $[\text{D}_6]\text{DMSO}$ ):  $\delta$  = 6.68 (d,  $J$  = 15.8 Hz, 1H; Ph-CH=CH-), 7.73 (d,  $J$  = 15.8 Hz, 1H; Ph-CH=CH-), 8.26 (s, 1H; arom. H), 12.84 ppm (brs, COOH);  $^{13}\text{C}$  NMR ( $[\text{D}_6]\text{DMSO}$ ):  $\delta$  = 124.78, 125.30, 126.57, 129.24, 129.71, 130.85, 136.59, 140.90, 166.59 ppm; MS:  $m/e$  found: 464.6744  $[\text{M}]^+$ ; calcd: 464.6812; elemental analysis calcd. (%) for  $\text{C}_9\text{H}_4\text{Br}_4\text{O}_2$ : C 23.31, H 0.87, Br 68.92; found: C 23.29, H 0.87, Br 68.88.

**Materials:** Native CK1 (nCK1) and CK2 (nCK2) were purified from rat liver.<sup>[45]</sup> Human recombinant  $\alpha$  and  $\beta$  subunits of CK2 were expressed in *E. coli* and the holoenzyme was reconstituted and purified as previously described.<sup>[44]</sup> V66A/I174A CK2 double mutant was obtained as previously described.<sup>[27,46]</sup> GSK3 $\beta$  was purchased from Upstate. DYRK1A was kindly provided by Dr. W. Becker (Aachen, Germany). The source of all the other protein kinases used for specificity assays is as previously either described or referenced.<sup>[30,47]</sup>

**Cell culture, treatment and viability assays:** The human leukemia Jurkat T-cell line was maintained in RPMI-1640, supplemented with foetal calf serum (10%, v/v), L-glutamine (2 mM), penicillin (100 units  $\text{mL}^{-1}$ ), and streptomycin (100  $\mu\text{g mL}^{-1}$ ). For the treat-

ment, cells were suspended at a density of  $10^6$  cells mL<sup>-1</sup> in a medium containing foetal calf serum (1%, v/v) and then incubated at 37 °C in the presence of the compounds at the indicated concentrations. Control cells were treated with equal amounts of solvent. At the end of incubations, cells were lysed by the addition of hypo-osmotic buffer, as previously described.<sup>[29]</sup> Cell viability was assessed with the aid of 3-(4,5-dimethylthiazol-2-yl)-3,5-diphenyl-triazolium bromide (MTT) reagent, while caspase activation was followed by Western blot monitoring of PARP and Hs1 protein degradation, as previously described.<sup>[32]</sup>

**Phosphorylation assays:** CK2 phosphorylation assays were carried out by incubation of the kinase (0.5–1 pmol) in the presence of increasing amounts of each inhibitor in a final mixture (25 µL) containing Tris-HCl (pH 7.5, 50 mM), NaCl (100 mM), MgCl<sub>2</sub> (12 mM), synthetic peptide substrate RRRADDSDDDDD (100 µM) and [ $\gamma$ -<sup>33</sup>P]-ATP] (0.02 mM, 500–1000 cpm pmol<sup>-1</sup>), unless otherwise indicated. After 10 min incubation at 37 °C the reaction was stopped by addition of orthophosphoric acid (5 µL of 0.5 M), after which aliquots were spotted onto phosphocellulose filters. Filters were washed four times in phosphoric acid (75 mM, 5–10 mL each) and then once in methanol and dried before counting. GSK3 $\beta$  activity was assayed by incubation for 10 min at 37 °C of the inhibitor-2 (2 µg) of protein phosphatase 1, as phosphorylatable substrate, in a mixture (25 µL) containing MOPS (8 mM), EDTA (0.2 mM), MgCl<sub>2</sub> (10 mM) and [ $\gamma$ -<sup>33</sup>P]-ATP (0.1 mM). Incorporated phosphate was determined by SDS-PAGE and autoradiography. Conditions for the activity assays of all other protein kinases are as previously described or referenced.<sup>[26,30,47]</sup>

**Kinetics:** Initial velocities were determined at each of the substrate concentrations tested. Inhibition data for a range of concentrations of each competitive inhibitor at a constant concentration of the nucleotide phosphate donor were plotted as a Dixon plot ([I] vs. 1/v) to give the IC<sub>50</sub> value at that concentration of S as the opposite value of the x intercept.<sup>[48]</sup>  $K_M$  values were calculated either in the absence or in the presence of increasing concentrations of inhibitor, from Lineweaver–Burk double-reciprocal plots of the data. Inhibition constants were then calculated by linear regression analysis of  $K_M/V_{max}$  versus inhibitor concentration plots. Inhibition constants were also deduced from the IC<sub>50</sub>/ $K_i$  Cheng–Prusoff relationship,<sup>[49]</sup> by determining the IC<sub>50</sub> value for each compound at 1 µM ATP concentration, assuming a competitive mechanism of inhibition.

**Molecular modelling:** All modeling studies were carried out on a 10 CPU (PIV-3.0GHZ and AMD64) Linux cluster running under openMosix architecture.<sup>[50]</sup>

**Target structures:** Human CK2  $\alpha$  subunit was retrieved from the PDB (PDB ID: 1JWH)<sup>[51]</sup> and processed to remove the ligands and water molecules. Hydrogen atoms were added to the protein structure by use of standard geometries with the MOE program.<sup>[52]</sup> To minimize contacts between hydrogens, the structures were subjected to Amber94<sup>[53]</sup> force field minimization until the rms of the conjugate gradient was < 0.1 kcal mol<sup>-1</sup> Å<sup>-1</sup> with the heavy atoms kept fixed at their crystallographic positions.

**Ligands:** The structures of all ATP-competitive inhibitor ligands were constructed with the aid of the Builder module in the MOE suite and minimized by use of the MMFF94<sup>[54]</sup> force field. Charges calculated by the AM1/ESP<sup>[54]</sup> method for the ligands were imported from the MOPAC<sup>[55]</sup> output files.

**Docking:** Ligands were docked into CK2 protein structure with the aid of the programs MOE-Dock<sup>[52]</sup> and GOLD (version 2.1).<sup>[56]</sup> For

the docking runs, all variable parameters had the default values. Only the top-ranked pose of each ligand obtained by both docking protocols was evaluated. MOE conformational samplings were conducted within a user-specified 3D docking box, by use of the Tabù Search protocol<sup>[57]</sup> and MMFF94 force field.<sup>[58]</sup> GOLD uses a genetic algorithm in its docking/scoring function and has five predefined speeds of operation. The work reported in this paper used only the fastest and slowest (standard default (SD) settings) of these five modes. A detailed analysis of the scoring functions is beyond the scope of this paper; however, GoldScore (rather than the alternative of ChemScore) was used to score the GOLD-docked poses and predicted pK<sub>i</sub> (rather than interaction energy) was used to score the MOE dockings.

**Abbreviations:** TBCA = tetrabromocinnamic acid. MAPK = mitogen-activated protein kinase. ERK = extracellular signal-regulated kinase. MKK = MAPK kinase (also called MEK). JNK = c-Jun N-terminal kinase. SAPK = stress-activated protein kinase. MAPKAP = MAPK-activated protein kinase. MSK = mitogen- and stress-activated protein kinase. PRAK = p38-regulated/activated kinase. PKA = cAMP-dependent protein kinase. PKC = protein kinase C. PDK = 3-phosphoinositide-dependent kinase. PKB = protein kinase B (also called Akt). SGK = serum- and glucocorticoid-induced kinase. S6K = ribosomal protein S6 kinase. GSK3 = glycogen synthase kinase-3. ROCK = Rho-dependent protein kinase. AMPK = AMP-activated protein kinase. CHK = checkpoint kinase. PHK = phosphorylase kinase. LCK = lymphocyte kinase. CSK = c-Src kinase. CDK = cyclin-dependent kinase. DYRK = dual-specificity tyrosine phosphorylation-regulated kinase.

## Acknowledgements

We thank Professor Sir Philip Cohen (Dundee, Scotland) for a critical reading of the manuscript. The work was supported by grants to L.A.P. and F.M. from the Italian Ministry for University and Research (MIUR; PRIN 2003 and 2004 and FIRB), AIRC and European Commission (PRO-KINASERESEARCH 503467). The molecular modelling work coordinated by S.M. was carried out with financial support from the University of Padova, Italy, and the MIUR, Rome, Italy. S.M. is also very grateful to Chemical Computing Group for the scientific and technical partnership.

**Keywords:** ATP mimetics • casein kinase • CK2 • inhibitors • structure–activity relationships

- [1] G. Manning, D. B. Whyte, R. Martinez, T. Hunter, S. Sudarsanam, *Science* **2002**, 298, 1912–1934.
- [2] S. Johnson, T. Hunter, *Nat. Methods* **2005**, 2, 17–25.
- [3] P. Blume-Jensen, T. Hunter, *Nature* **2001**, 411, 355–365.
- [4] P. Cohen, *Nat. Rev. Drug Discovery* **2002**, 1, 309–315.
- [5] A. L. Hopkins, C. R. Groom, *Nat. Rev. Drug Discovery* **2002**, 1, 727–730.
- [6] C. L. Sawyers, *Curr. Opin. Genet. Dev.* **2002**, 12, 111–115.
- [7] A. L. Hannah, *Curr. Mol. Med.* **2005**, 5, 625–642.
- [8] D. Fabbro, C. Garcia-Echeverria, *Curr. Opin. Drug Discovery Dev.* **2002**, 5, 701–712.
- [9] *Handbook of Experimental Pharmacology*, Vol. 167 (Eds.: L. A. Pinna, P. T. W. Cohen), Springer, Berlin, **2005**.
- [10] B. J. Druker, M. Talpaz, D. J. Resta, B. Peng, E. Buchdunger, J. M. Ford, N. B. Lydon, H. Kantarjian, R. Capdeville, S. Ohno-Jones, C. L. Sawyers, *N. Engl. J. Med.* **2001**, 344, 1031–1037.
- [11] F. Meggio, L. A. Pinna, *FASEB J.* **2003**, 17, 349–368.
- [12] L. A. Pinna, *Biochim. Biophys. Acta* **1990**, 1054, 267–284.
- [13] L. A. Pinna, *J. Cell Sci.* **2002**, 115, 3873–3878.
- [14] L. A. Pinna, *Acc. Chem. Res.* **2003**, 36, 378–384.

- [15] D. W. Litchfield, *Biochem. J.* **2003**, 369, 1–15.
- [16] S. Tawfic, S. Yu, H. Wang, R. Faust, A. Davis, K. Ahmed, *Histol. Histopathol.* **2001**, 16, 573–582.
- [17] G. M. Unger, A. T. Davis, J. W. Slaton, K. Ahmed, *Curr. Cancer Drug Targets* **2004**, 4, 77–84.
- [18] D. C. Seldin, P. Leder, *Science* **1995**, 267, 894–897.
- [19] M. A. Kelliher, D. C. Seldin, P. Leder, *EMBO J.* **1996**, 15, 5160–5166.
- [20] E. Landesman-Bollag, P. L. Channavajhala, R. D. Cardiff, D. C. Seldin, *Oncogene*, **1998**, 16, 2965–2974.
- [21] M. Orlandini, F. Semplici, R. Ferruzzi, F. Meggio, L. A. Pinna, S. Oliviero, *J. Biol. Chem.* **1998**, 273, 21291–21297.
- [22] K. Ahmed, D. A. Gerber, C. Cochet, *Trends Cell Biol.* **2002**, 12, 226–230.
- [23] K. A. Ahmad, G. Wang, J. Slaton, G. Unger, K. Ahmed, *Anticancer Drugs* **2005**, 16, 1037–1043.
- [24] G. Wang, G. Unger, K. A. Ahmad, J. W. Slaton, K. Ahmed, *Mol. Cell. Biochem.* **2005**, 274, 77–84.
- [25] H. Yim, Y. H. Lee, C. H. Lee, S. K. Lee, *Planta* **1999**, 65, 9–13.
- [26] F. Meggio, M. A. Pagano, S. Moro, G. Zagotto, M. Ruzzene, S. Sarno, G. Cozza, J. Bain, M. Elliott, A. Donella Deana, A. M. Brunati, L. A. Pinna, *Biochemistry* **2004**, 43, 12931–12936.
- [27] M. A. Pagano, M. Andrzejewska, M. Ruzzene, S. Sarno, L. Cesaro, J. Bain, M. Elliott, F. Meggio, Z. Kazimierczuk, L. A. Pinna, *J. Med. Chem.* **2004**, 47, 6239–6247.
- [28] E. Vangrevelinghe, K. Zimmermann, J. Schoepfer, R. Portmann, D. Fabbro, P. Furet, *J. Med. Chem.* **2003**, 46, 2656–2662.
- [29] S. Sarno, E. De Moliner, M. Ruzzene, M. A. Pagano, R. Battistutta, J. Bain, D. Fabbro, J. Schoepfer, M. Elliott, P. Furet, F. Meggio, G. Zanotti, L. A. Pinna, *Biochem. J.* **2003**, 374, 639–646.
- [30] S. P. Davies, H. Reddy, M. Caivano, P. Cohen, *Biochem. J.* **2000**, 351, 95–105.
- [31] S. Sarno, M. Salvi, R. Battistutta, G. Zanotti, L. A. Pinna, *Biochim. Biophys. Acta* **2005**, 1754, 263–270.
- [32] M. Ruzzene, D. Penzo, L. A. Pinna, *Biochem. J.* **2002**, 364, 41–47.
- [33] S. Mishra, A. Reichert, J. Cunnick, D. Senadheera, B. Hemmeryckx, N. Heisterkamp, J. Groffen, *Oncogene*, **2003**, 22, 8255–8262.
- [34] P. Zien, J. S. Duncan, J. Skierski, M. Bretner, D. W. Litchfield, D. Shugar, *Biochim. Biophys. Acta* **2005**, 1754, 271–280.
- [35] M. A. Pagano, F. Meggio, M. Ruzzene, M. Andrzejewska, Z. Kazimierczuk, L. A. Pinna, *Biochem. Biophys. Res. Commun.* **2004**, 321, 1040–1044.
- [36] R. Battistutta, S. Sarno, E. De Moliner, E. Papinutto, G. Zanotti, L. A. Pinna, *J. Biol. Chem.* **2000**, 275, 29618–29622.
- [37] R. Battistutta, E. De Moliner, S. Sarno, G. Zanotti, L. A. Pinna, *Protein Sci.* **2001**, 10, 2200–2206.
- [38] E. De Moliner, S. Moro, S. Sarno, G. Zagotto, G. Zanotti, L. A. Pinna, R. Battistutta, *J. Biol. Chem.* **2003**, 278, 1831–1836.
- [39] R. Battistutta, M. Mazzorana, S. Sarno, Z. Kazimierczuk, G. Zanotti, L. A. Pinna, *Chem. Biol.* **2005**, 12, 1211–1219.
- [40] X. Altafaj, M. Dierssen, C. Baamonde, E. Marti, J. Visa, J. Guimera, M. Oset, J. R. Gonzalez, J. Florez, C. Fillat, X. Estivill, *Hum. Mol. Genet.* **2001**, 10, 1915–1923.
- [41] B. Hammerle, A. Carnicero, C. Elizalde, J. Ceron, S. Martinez, F. J. Tejedor, *Eur. J. Neurosci.* **2003**, 17, 2277–2286.
- [42] I. Ferrer, M. Barrachina, B. Puig, M. Martinez de Lagran, E. Marti, J. Avila, M. Dierssen, *Neurobiol. Dis.* **2005**, 20, 392–400.
- [43] G. Lock, *Monatsh. Chem.* **1959**, 90, 683–687.
- [44] O. Bayer, *Houben-Weyl—Methoden der Organischen Chemie, Band VII, Teil 1 (Aldehyde)*, **1954**, 143–144.
- [45] F. Meggio, A. Donella Deana, L. A. Pinna, *J. Biol. Chem.* **1981**, 256, 11958–11961.
- [46] S. Sarno, P. Vaglio, F. Meggio, O.-G. Issinger, L. A. Pinna, *J. Biol. Chem.* **1996**, 271, 10595–10601.
- [47] J. Bain, H. McLauchlan, M. Elliott, P. Cohen, *Biochem. J.* **2003**, 371, 199–204.
- [48] B. T. Burlingham, T. S. Widlanski, *J. Chem. Educ.* **2003**, 80, 214–218.
- [49] Y.-C. Cheng, W. H. Prusoff, *Biochem. Pharmacol.* **1973**, 22, 3099–3108.
- [50] OpenMosix: <http://www.openMosix.org> (**2004**).
- [51] H. M. Berman, J. Westbrook, Z. Feng, G. Gilliland, T. N. Bhat, H. Weissig, I. N. Shindyalov, P. E. Bourne, *Nucleic Acids Res.* **2000**, 28, 235–242.
- [52] MOE (The Molecular Operating Environment) Version 2005.06, software available from Chemical Computing Group Inc., 1010 Sherbrooke Street West, Suite 910, Montreal, Canada H3A 2R7. <http://www.chemcomp.com>.
- [53] D. A. Case, T. E. Cheatham III, T. Darden, H. Gohlke, R. Luo, K. M. Merz, Jr., A. Onufriev, C. Simmerling, B. Wang, R. Woods, *J. Comput. Chem.* **2005**, 26, 1668–1688.
- [54] B. H. Besler, K. M. Merz, P. A. Kollman, *J. Comput. Chem.* **1990**, 11, 431–439.
- [55] MOPAC 7, J. J. P. Stewart, **1993**, Fujitsu Limited, Tokyo, Japan.
- [56] G. Jones, P. Willett, R. C. Glen, A. R. Leach, R. Taylor, *J. Mol. Biol.* **1997**, 267, 727–748.
- [57] C. A. Baxter, C. W. Murray, D. E. Clark, D. R. Westhead, M. D. Eldridge, *Proteins Struct. Funct. Genet.* **1998**, 33, 367–382.
- [58] T. Halgren, *J. Comput. Chem.* **1996**, 17, 490–519.

Received: July 14, 2006

Published online on November 29, 2006